Available online at www.sciencedirect.com
SCIENCE DIRECT®
Journal of Crystal Growth 281 (2005) 475–480
JOURNAL OF CRYSTAL GROWTH
www.elsevier.com/locate/jcrysgro

Post-annealing of Al-doped ZnO films in hydrogen atmosphere

Byeong-Yun Oh, Min-Chang Jeong, Doo-Soo Kim, Woong Lee, Jae-Min Myoung*

Information & Electronic Materials Research Laboratory, Department of Materials Science and Engineering, Yonsei University, 134 Shinchon-dong, Seoul 120-749, Korea

Received 9 March 2005; accepted 14 April 2005
Available online 24 May 2005
Communicated by D.P. Norton

Abstract

Electrical properties of ZnO:Al films deposited on glass substrates by RF magnetron co-sputtering method have been modified by post-deposition annealing treatment in hydrogen atmosphere for potential transparent conductive oxide (TCO) applications. Annealing treatments were carried out at 573 K for compatibility with typical display device fabrication processes and annealing time was varied between 10 and 120 min. Whereas there were no significant changes in crystallinity of the films, resistivity decreased from 4.80×10^{-3} to $8.30 \times 10^{-4}\,\Omega\,\mathrm{cm}$ and carrier concentration increased from 2.11×10^{20} to $8.86 \times 10^{20}\,\mathrm{cm}^{-3}$ when annealing time was 60 min. Improved electrical properties are ascribed to desorption of the negatively charged oxygen species from the grain boundary surfaces by the hydrogen annealing treatment. The optical properties of the films, which change in accordance with the Burstein–Moss effect, are consistent with the observed changes in electrical properties.

PACS: 73.61.Ga; 73.25.+i; 73.61.−r; 78.66.+m

Keywords: A1. Hydrogen passivation; B1. Al-doped ZnO (ZnO:Al); B1. Transparent conductive oxide (TCO)

1. Introduction

Transparent conductive oxide (TCO) films such as indium oxide-based and zinc oxide-based TCOs have been widely studied for potential applications in flat panel displays, solar cells and organic light-emitting diodes exploiting their high-luminous transmittance and good electrical conductivities [1–5]. In particular, ZnO films doped with an n-type dopant Al are regarded as good substitutes for indium tin oxide (ITO), especially due to thermal stability and relatively lower cost [6–8]. The electrical properties of ZnO:Al films for TCO applications, resistivity in particular, should be

*Corresponding author. Tel.: +82 2 2123 2843; fax: +82 2 365 2680.
E-mail address: jmmyoung@yonsei.ac.kr (J.-M. Myoung).

0022-0248/$ - see front matter © 2005 Elsevier B.V. All rights reserved.
doi:10.1016/j.jcrysgro.2005.04.045

comparable to ITO films, while mass production by simple process should be possible. However, electrical properties of ZnO:Al films reported so far are not satisfactory in many cases [9–11]. Rather poorer electrical properties of ZnO:Al films are mainly due to depletion regions formed by the adsorption of negatively charged species on grain boundary surfaces [12–14]. It is known that hydrogen plays a beneficial role in removing such depletion regions [8,15–18]. Therefore, efforts have been made to eliminate the depletion regions by employing various treatments with hydrogen [19–21]. Among these, post-deposition annealing in hydrogen atmosphere seems to be an attractive way of achieving property enhancements, as it is a simple low-cost process. It has been reported that electrical properties could be improved significantly by increasing annealing temperature [8,18,22,23]. However, high-annealing temperature may damage the glass substrate and the device structures such as display device and solar cell applications during the annealing process. As an alternative, in this study, low-temperature annealing process was attempted by choosing the annealing time as controlled variable. It is expected that only electrical properties would be improved without noticeable changes in crystallinity of ZnO:Al films by the annealing process at low temperature.

2. Experimental procedure

ZnO:Al thin films were deposited on glass substrates by RF magnetron co-sputtering using a ZnO target (5N) and an Al target (5N). Glass substrates were cleaned with standard cleaning procedure and then loaded in the central region of the substrate holder located 50 mm away from the targets. While the sputtering chamber was initially evacuated to the base pressure of about 7.5×10^{-4} Pa, the working pressure for film deposition was maintained at 0.67 Pa with Ar ambient gas. Prior to the film deposition, pre-sputtering was performed for 10 min to remove any contaminants on the target surfaces. ZnO:Al films were then grown at room temperature with the ZnO RF power of 165 W and the Al RF power of 90 W. As-deposited ZnO:Al films were subsequently heat-treated in hydrogen atmosphere by varying the annealing time between 10 and 120 min at the annealing temperature of 573 K. This temperature was chosen since it is known as the allowed maximum in typical device processing. It was also expected that this annealing temperature was not high enough to cause significant re-crystallization of the films so that only the effect of hydrogen treatment could be investigated [22,23]. Crystallinity of the hydrogen-annealed ZnO:Al films was investigated by X-ray diffraction (XRD) in $\theta - 2\theta$ scan mode using a Ni-filtered CuK_α source. Surface morphology of the films was observed by atomic force microscope (AFM). The Al contents of the ZnO:Al films were ~2.85 wt% measured by energy dispersive X-ray spectrometer (EDS). Electrical properties of the hydrogen-annealed ZnO:Al films were measured by van der Pauw method at room temperature and a spectrophotometer was used for measuring the optical properties of the films in the wavelength range of 300–700 nm.

3. Results and discussion

Fig. 1 shows the XRD spectra of the ZnO:Al films heat-treated in hydrogen atmosphere for various annealing times. It is noticed that all the films exhibit only the ZnO (0 0 2) peaks, indicating that the films have *c*-axis preferred orientation due to self-texturing phenomenon [24]. The values of full-width at half-maximum (FWHM) of the ZnO (0 0 2) peaks were ~0.27° for all films, suggesting that the hydrogen annealing did not cause noticeable changes in the crystallinity of the films. It was also observed that there are shifts of the position of the ZnO (0 0 2) peaks toward higher diffraction angles from 34.32° to 34.36° as annealing time in hydrogen atmosphere increased, implying relaxation of the residual strain introduced in the films during the deposition process [8,17,22]. In-plane biaxial stresses in the ZnO:Al films were estimated using the formula: $\sigma = -453.6 \times 10^9 (c - c_0)/c_0$ where c is the c-axis lattice constant obtained from the peak positions in Fig. 1 and c_0 (= 0.52066) is the strain-free c-axis lattice constant of

ZnO [23]. The estimated in-plane biaxial stresses in the films decreased from −1.42 to −0.91 GPa with increasing annealing time showing only slight relaxation of the residual stress. It is, therefore, expected that effect of stress relief during the post-annealing process does not have significant effect on the electrical and optical properties of the ZnO:Al films.

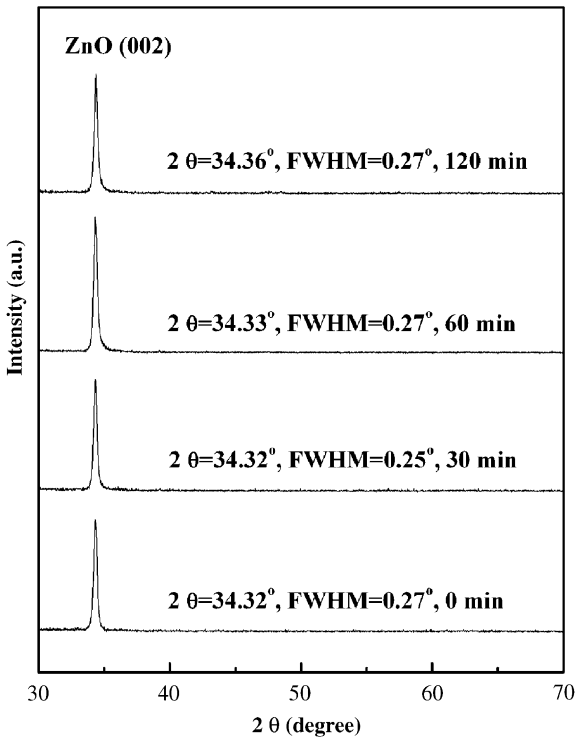

Fig. 1. XRD spectra of the ZnO:Al films annealed in hydrogen atmosphere for different annealing times.

Change in the surface morphology of the ZnO:Al films after the hydrogen annealing treatment was subsequently investigated using an AFM and the resulting surface images are shown in Fig. 2 for various annealing times. The measured root-mean-square (RMS) roughnesses were 1.94, 2.34, 2.75, and 2.73 nm for the samples annealed for 0 (as-deposited), 30, 60, and 120 min, respectively. It is known that the increase in surface roughness may cause deterioration of the electrical and optical properties [14,25]. However, as will be shown below, these differences in the RMS roughness do not seem to have significant influence on the electrical and optical properties of the films considered in this study. Therefore, together with the XRD results, it is suggested that the improvement in electrical and optical properties of the ZnO:Al films would be due to the favorable role of hydrogen.

Changes in the electrical properties of the ZnO:Al films are shown in Fig. 3 as the function of hydrogen annealing time. The electrical properties of the ZnO:Al films improved with increasing annealing time to 60 min and then remained almost unchanged thereafter. Electrical resistivity

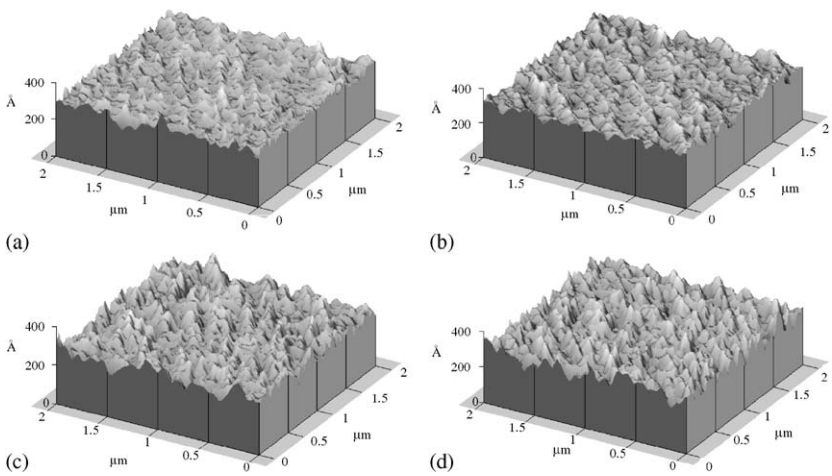

Fig. 2. AFM images of ZnO:Al films over 2 μm × 2 μm area: (a) as-deposited and annealed in hydrogen atmosphere for (b) 30 min, (c) 60 min, and (d) 120 min.

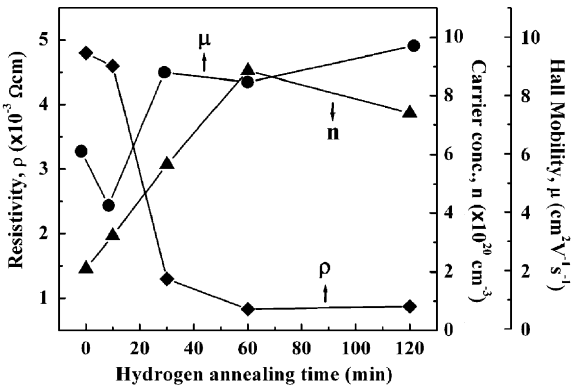

Fig. 3. Changes in the electrical resistivity and the carrier concentration of the ZnO:Al films with varying hydrogen annealing time.

and carrier concentration of the as-deposited ZnO:Al film were measured to be $4.80 \times 10^{-3}\,\Omega$cm and $2.11 \times 10^{20}\,\mathrm{cm}^{-3}$, respectively. Then, the resistivity of the hydrogen-annealed film decreased to $8.30 \times 10^{-4}\,\Omega\,\mathrm{cm}$, which is accompanied by the increase in the carrier concentration to $8.86 \times 10^{20}\,\mathrm{cm}^{-3}$, with the annealing time of 60 min. Further extending the annealing time did not result in noticeable changes in both the resistivity and the carrier concentration. Regarding the carrier mobility, as shown in Fig. 3, it increases from 6.09 in the as-deposited film to $9.70\,\mathrm{cm}^2\,\mathrm{V}^{-1}\,\mathrm{s}^{-1}$ in the hydrogen-annealed film. In general, resistivity of the films is mainly affected by carrier concentration and mobility. Since the increase of the carrier mobility (160%) shown in Fig. 3 was small compared to the increase of carrier concentration (420%), the improved electrical property is mainly due to the increase in carrier concentration.

In the current ZnO:Al films, such increase in carrier concentration is attributed to the desorption of negatively charged oxygen species from the grain boundaries which act as trapping sites and form the potential barriers during the hydrogen treatment [12,15]. The negatively charged species form depletion regions near the grain boundary surfaces decreasing free-carrier concentration and Hall mobility. If these depletion regions in the ZnO:Al films were removed by the passivation of the grain boundary surfaces during the post-deposition annealing in hydrogen atmosphere, carrier concentration and Hall mobility would increase. Since the Al contents in the films did not change during the annealing process, as mentioned above, it is believed that passivation of grain boundary surfaces by hydrogen is the main reason for the improved electrical properties [13,17]. Electrical properties of the hydrogen-annealed ZnO:Al films remained unchanged after 40 days in atmosphere, indicating that the hydrogen passivated grain boundary surfaces are stable [13].

Transmittance of the as-deposited and the hydrogen-annealed ZnO:Al films was measured at room temperature and the resulting spectra are shown in Fig. 4. It can be seen that the average optical transmittance in the visible light wavelength range is over 90% that of the glass substrate for all the samples. The optical bandgap energies of the films estimated from the absorption edges are large compared to that of undoped ZnO (3.30 eV) increasing from 3.54 to 3.70 eV as the annealing time increases from 0 to 60 min and over [6]. The blueshift of the absorption edges with increasing annealing time to 60 min is attributed to Burstein–Moss effect [26,27]. According to the Burstein–Moss effect, the increase of the Fermi level in the conduction band leads to the bandgap energy broadening with increasing carrier concentration. The bandgap energy

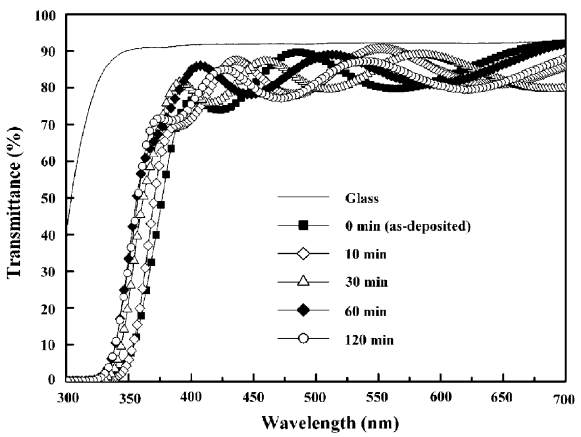

Fig. 4. Optical transmittance spectra of the ZnO:Al films as-deposited and hydrogen-annealed for various annealing times.

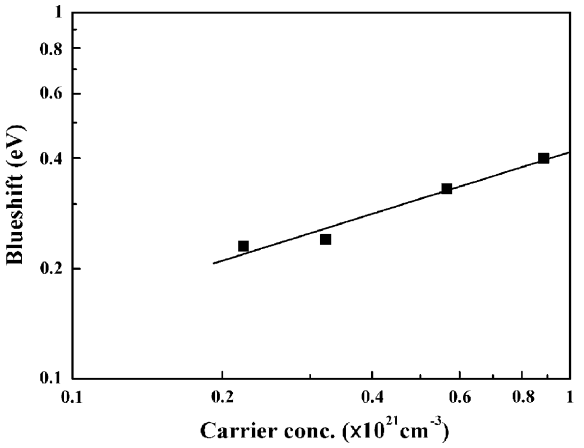

Fig. 5. Relation between the optical bandgap energy widening and the carrier concentration.

broadening (ΔE_g) is expressed as

$$\Delta E_g = \frac{h^2}{8m^*}\left(\frac{3}{\pi}\right)^{2/3} n_e^{2/3}, \quad (1)$$

where h is Planck's constant, m^* is the electron effective mass in conduction band, and n_e is carrier concentration. Fig. 5 shows the blueshift in the optical bandgap energy of the ZnO:Al films as function of the carrier concentration [28,29]. Assuming that the exponent of the carrier concentration n_e is unknown, substituting measured values of ΔE_g and n_e into Eq. (1) gives the exponent of 0.655. This shows that the optical bandgap energy obtained for these ZnO:Al films follows the Burstein–Moss effect without the many-body perturbation effect [30,31]. These optical properties related to bandgap energy of the ZnO:Al films have good correlation with their electrical properties shown in Fig. 3. The results so far suggest that the electrical and optical properties of the ZnO:Al films can be improved for TCO applications by controlling the time of post-deposition annealing in hydrogen atmosphere at relatively low temperature.

4. Conclusions

Time-controlled low-temperature annealing process on ZnO:Al films in hydrogen atmosphere was introduced in this study for the purpose of improving their electrical properties for potential optoelectronic device applications. Changes in the crystalline, electrical, and optical properties of the co-sputtered ZnO:Al films after the heat treatment in hydrogen atmosphere were studied as the function of the annealing time. Substantial improvement in the electrical properties could be achieved by increasing the annealing time without noticeable changes in the crystallinity of the c-axis oriented wurtzite ZnO:Al films. However, once the resistivity reached the minimum of $8.30 \times 10^{-4}\,\Omega\,\mathrm{cm}$, further increasing the annealing time did not result in the additional improvement in the electrical properties. Reduced resistivity of the ZnO:Al films is attributed to the increased free carrier concentrations from 2.11×10^{20} to $8.86 \times 10^{20}\,\mathrm{cm}^{-3}$ and Hall mobility from 6.09 to $9.70\,\mathrm{cm}^2\,\mathrm{V}^{-1}\,\mathrm{s}^{-1}$, which originated from the desorption of the negatively charged oxygen species from the grain boundary surfaces by the hydrogen treatment. Blueshift of the absorption edges in transmittance spectra with increasing annealing time, which is attributed to the Burstein–Moss effect, supports the observed changes in electrical properties. It is, therefore, suggested that the method presented in this study would be an effective way of modifying the electrical properties of ZnO:Al TCO films that can be applied to device fabrication process with relative ease.

References

[1] C.C. Wu, C.I. Wu, J.C. Sturm, A. Kahn, Appl. Phys. Lett. 70 (1997) 1348.
[2] G.S. Chae, Jpn. J. Appl. Phys. 40 (2001) 1282.
[3] K. Matsubara, P. Fons, K. Iwata, A. Yamada, K. Sakurai, H. Tampo, S. Niki, Thin Solid Films 431–432 (2003) 369.
[4] H. Kim, J.S. Horwitz, G.P. Kushto, Z.H. Kafafi, D.B. Chrisey, Appl. Phys. Lett. 79 (2001) 284.
[5] F. Li, H. Tang, J. Shinar, O. Resto, S.Z. Weisz, Appl. Phys. Lett. 70 (1997) 2741.
[6] B.Y. Oh, M.C. Jeong, W. Lee, J.M. Myoung, J. Crystal Growth 274 (2005) 453.
[7] T. Minami, T. Miyata, T. Yamamoto, J. Vac. Sci. Technol. A 17 (1999) 1822.
[8] J.F. Chang, W.C. Lin, M.H. Hon, Appl. Surf. Sci. 183 (2001) 18.
[9] S.S. Lin, J.L. Huang, P. Sajgalik, Surf. Coat Technol. 185 (2004) 254.

[10] S.H. Jeong, J.W. Lee, S.B. Lee, J.H. Boo, Thin Solid Films 435 (2003) 78.
[11] Y. Zhou, P.J. Kelly, A. Postill, O. Abu-Zeid, A.A. Alnajjar, Thin Solid Films 447–448 (2004) 33.
[12] Y. Takahashi, M. Kanamori, A. Kondoh, H. Minoura, Y. Ohya, Jpn. J. Appl. Phys. 33 (1994) 6611.
[13] M.L. Addonizio, A. Antonaia, G. Cantele, C. Privato, Thin Solid Films 349 (1999) 93.
[14] S.Y. Myong, K.S. Lim, Appl. Phys. Lett. 82 (2003) 3026.
[15] V. Srikant, D.R. Clarke, J. Appl. Phys. 81 (1997) 6357.
[16] S.J. Baik, J.H. Jang, C.H. Lee, W.Y. Cho, K.S. Lim, Appl. Phys. Lett. 70 (1997) 3516.
[17] T. Tsuji, M. Hirohashi, Appl. Surf. Sci. 157 (2000) 47.
[18] S.A. Studenikin, N. Golego, M. Cocivera, J. Appl. Phys. 87 (2000) 2413.
[19] K. Zhang, F. Zhu, C.H.A. Huan, A.T.S. Wee, J. Appl. Phys. 86 (1999) 974.
[20] Z. Zhou, K. Kato, T. Komaki, M. Yoshino, H. Yukawa, M. Morinaga, K. Morita, J. Eur. Ceram. Soc. 24 (2004) 139.
[21] B. Theys, V. Sallet, F. Jomard, A. Lusson, J.F. Rommeluere, Z. Teukam, J. Appl. Phys. 91 (1997) 3922.
[22] V. Gupta, A. Mansingh, J. Appl. Phys. 80 (1996) 1063.
[23] M.K. Puchert, P.Y. Timbrell, R.N. Lamb, J. Vac. Sci. Technol. A 14 (1996) 2220.
[24] X. Jiang, C.L. Jia, B. Szyszka, Appl. Phys. Lett. 80 (2002) 3090.
[25] K. Zhang, A.R. Forouhi, I. Bloomer, J. Vac. Sci. Technol. A 17 (1999) 1843.
[26] P.K. Chakraborty, G.C. Datta, K.P. Ghatak, Physica B 339 (2003) 198.
[27] Z.C. Jin, I. Hamberg, C.G. Granqvist, J. Appl. Phys. 64 (1988) 5117.
[28] M. Chen, Z.L. Pei, X. Wang, C. Sun, L.S. Wen, J. Vac. Sci. Technol. A 19 (2001) 963.
[29] K.H. Kim, K.C. Park, D.Y. Ma, J. Appl. Phys. 81 (1997) 7764.
[30] P.A. Wolff, Phys. Rev. 126 (1962) 405.
[31] B.E. Selnelius, K.F. Berggren, Z.C. Jin, I. Hamberg, C.G. Granqvist, Phys. Rev. B 37 (1988) 10244.